ARMA 19–13

Effects of Longwall-Induced Subsurface Deformations and Permeability Changes on Shale Gas Well Integrity and Safety under Shallow Cover

D. W.H. Su, P. Zhang, H. Dougherty, M. Van Dyke, T. Minoski (Ground Control Branch)

S. Schatzel, V. Gangrade, E. Watkins, J. Addis, C. Hollerich (Fires and Explosions Branch)

Centers for Disease Control and Prevention (CDC), National Institute for Occupational Safety and Health (NIOSH), Pittsburgh Mining Research Division (PMRD), Pittsburgh, PA 15236

ABSTRACT

This paper presents the results of a 2018 NIOSH (National Institute for Occupational Safety and Health) study to evaluate longwall-induced subsurface deformations and permeability changes and their effects on shale gas well integrity and safety under shallow cover. A study site was selected over a southwestern Pennsylvania coal mine, which extracts 457-meter-wide longwall faces under 147 meters of cover. One in-place inclinometer (IPI) well and three permeability monitoring wells were drilled and installed over a 38-m by 84-m centers abutment pillar. In addition to the inclinometer well and monitoring wells, surface subsidence measurements and underground coal pillar pressure measurements were conducted as the first 457-meter-wide longwall panel on the south side of the abutment pillar mined by.

Comparisons of a series of FLAC3D finite difference simulation results and the surface, subsurface, and underground instrumentation results show that the measured IPI casing deformations are in reasonable agreement with those predicted by the FLAC3D models, and that the measured surface subsidence and pillar pressure are in excellent agreement with those predicted by the 3D models. Measured permeability changes were incorporated into a preliminary calculation to evaluate the effect of a hypothetical shale gas well leak on longwall ventilation, which indicates negligible impact after completion of first panel mining. Results from this 2018 research clearly indicate that under shallow cover, the measured horizontal displacements within the abutment pillar are at least one order of magnitude higher than those measured in a 2017 study under deep cover and slightly higher than those measured in a 2014 study under medium cover.

INTRODUCTION

Due to a recent shale gas boom, approximately 1,500 unconventional shale gas wells have been drilled through active and future coal reserves in Pennsylvania, West Virginia, and Ohio over the past 15 years. These shale gas wells have penetrated many mineable coal seams, in

particular, the Pittsburgh Seam. These unconventional gas wells, whether tapped into the Marcellus or Utica formations, contain very high gas pressure. Strata deformations associated with longwall extractions could induce high stresses and deformations in the shale gas well casings, which may compromise the mechanical integrity of the production, intermediate, and coal protection casings (Figure 1). Damaged well casings could potentially introduce high-pressure, high volume explosive gas into underground mine workings, particularly during an extended well shut-in period, which could seriously jeopardize underground miners' safety and health.

In 2012, the Pennsylvania Department of Environmental Protection (PADEP) initiated a call for research to update the department's Gas Well Pillar Regulations (Commonwealth of Pennsylvania, 1957), which have been widely used by the Mine Safety and Health Administration (MSHA) and other states to govern gas well pillar stability issues over the past 60 years. In response to this call for research, a comprehensive study was conducted in a southwestern Pennsylvania coal mine by CONSOL Energy, the Marcellus Shale Coalition, and the Pennsylvania Coal Association to evaluate the effect of longwall-induced subsurface strata deformations on well casings above the mining horizon under 183 meters of cover (Su, 2016). Unfortunately, although it shed some lights on potential impact of longwall-induced deformations on gas well casing stability, this comprehensive study was so site-specific and could not be adopted as general guidelines. To provide additional critical scientific data, NIOSH initiated a research project in 2017 to evaluate the effects of longwall-induced deformations on shale gas well casing stability under deep as well as shallow covers. The effects of longwall-induced subsurface deformations on shale gas well casing stability under deep cover was presented in the 52nd ARMA and 37th International Ground Control Conferences (Su, et al., 2018a; Su, et al., 2018b). This paper presents the results from a recent NIOSH research study focusing on the longwall-induced subsurface deformations and permeability changes under a shallow stream valley environment.

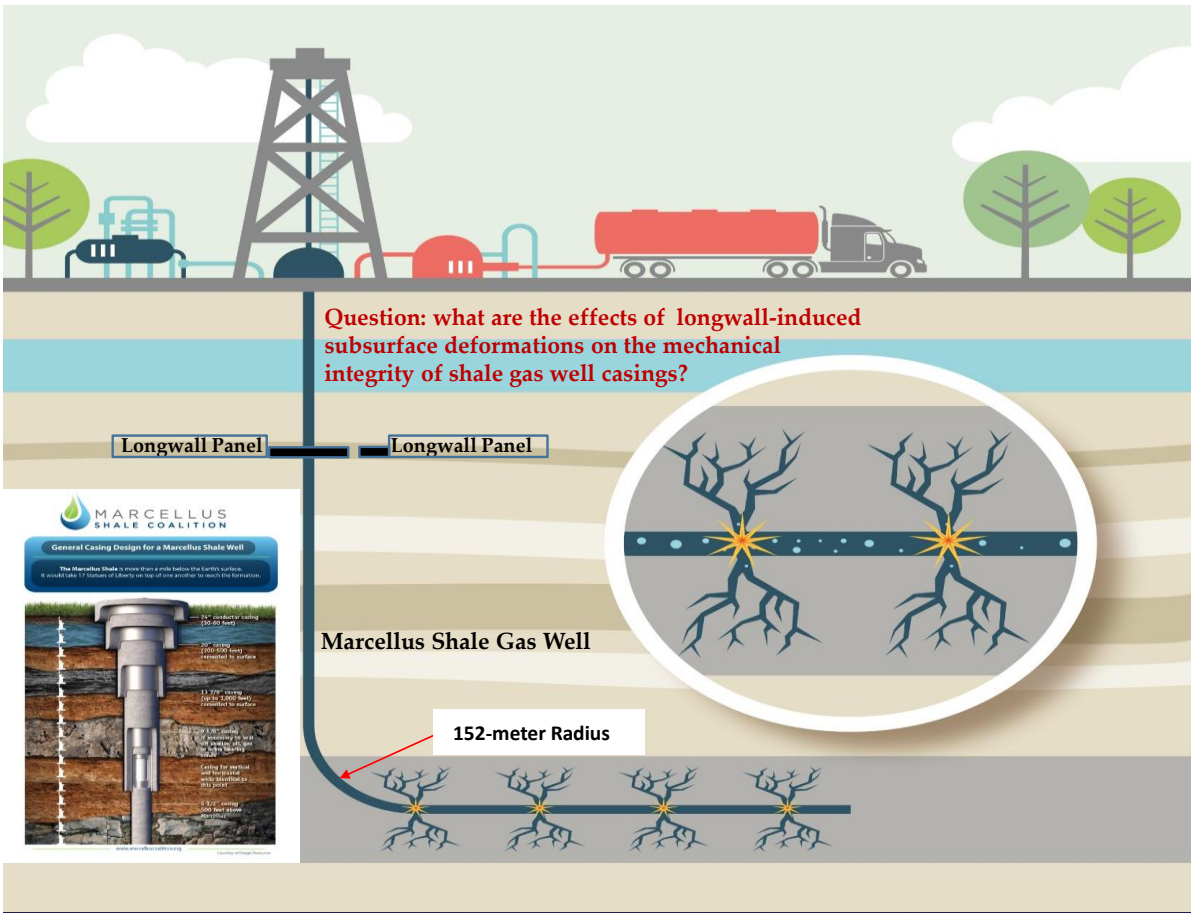

Figure 1. Shale gas well penetrating a longwall abutment pillar and typical five-casing well design.

SITE DESCRIPTION AND GEOTECHNICAL INSTRUMENTATIONS

The study site was located over a southwestern Pennsylvania coal mine employing 457-meter-wide longwall panels to extract coal from the Pittsburgh seam, which lies 147 meters below the surface. A three-entry longwall gate-road system of 18.3-m X 38-m centers was employed at the mine. Figure 2 illustrates the layout of the longwall panels, which are oriented approximately in the east-west direction. Figure 2 also shows the locations of the surface and subsurface instrumentation layout, which includes one 143-meter-deep subsurface inclinometer monitoring hole and three permeability monitoring holes drilled over the center of the 38-m x 84-m centers abutment pillar, and four borehole pressure cells installed into the 38-m x 84-m centers abutment pillar. Permeability holes FEB1, FEB2, and FEB3 were drilled to depths of 125, 79, and 41 meters, respectively. All permeability monitoring holes were cased and cemented from the surface down to the last 6.1 meters, where the casing was slotted and not cemented. In addition to the subsurface and underground measurements, pre- and post-longwall surface subsidence measurements were conducted to corroborate surface responses with subsurface and underground responses. The first panel approached and mined by the test site on July

13, 2018, and the second panel is expected to approach and mine by the test site in May 2019.

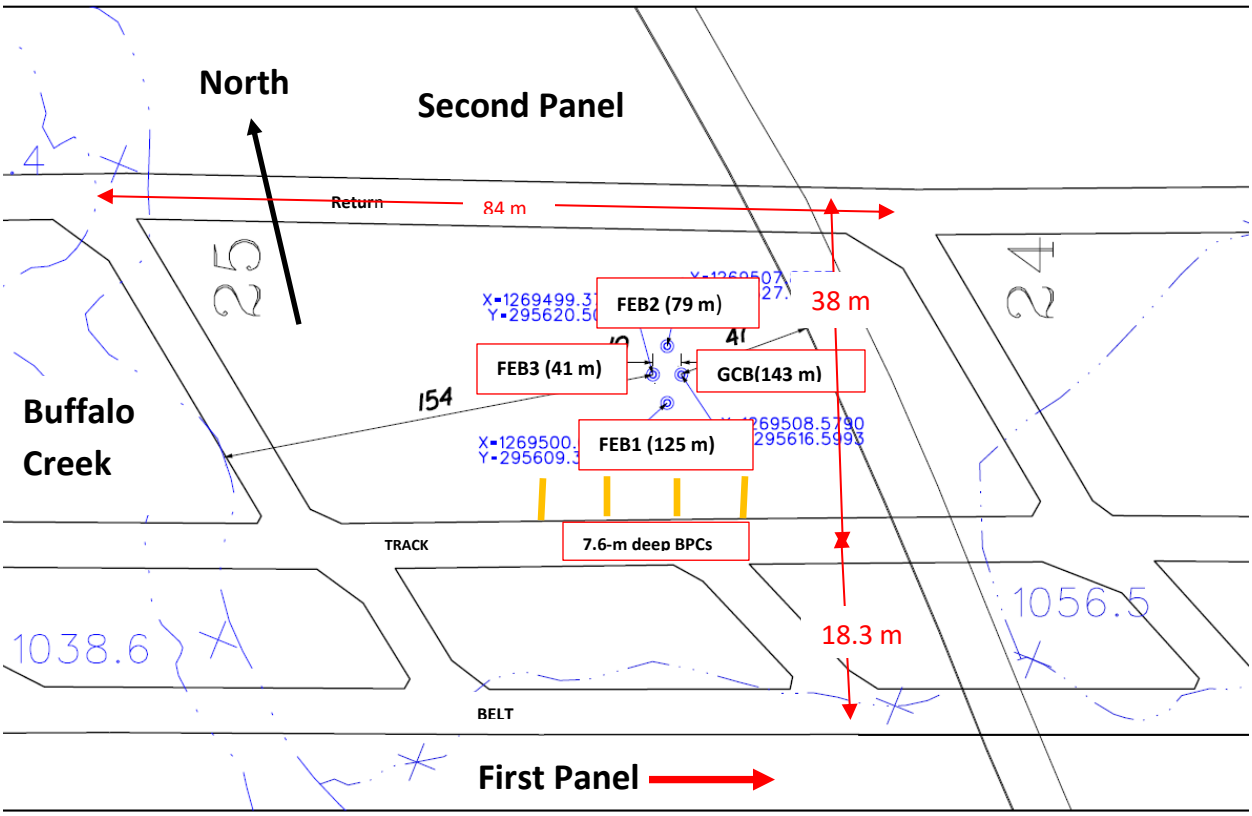

Figure 2. Surface and subsurface instrumentation layout.

SITE GEOLOGY

The overburden depth at the test site is 147 meters. Figure 3 shows the detailed overburden geology at the test site down to 143 meters below the surface, which has been interpreted by correlating a test site gamma log and a nearby core hole. Figure 3 shows that the overburden geology within the inclinometer monitoring zone contains many strong-to-weak rock interfaces, which have been demonstrated to have major influences on longwall-induced stresses and deformations from previous ground control research. In particular, the presence of weak Uniontown Coal zone above the A-, B-, C-, D-Limestone sequence at the 85-meter depth, and the presence of clayey shale in the suspected Sewickley Coal Zone sandwiched between the Benwood Limestone and the Sewickley Limestone at the 122-meter depth indicate potential planes of weakness where substantial longwall-induced subsurface bedding plane movements may occur.

Figure 3. Overburden geology at the test site.

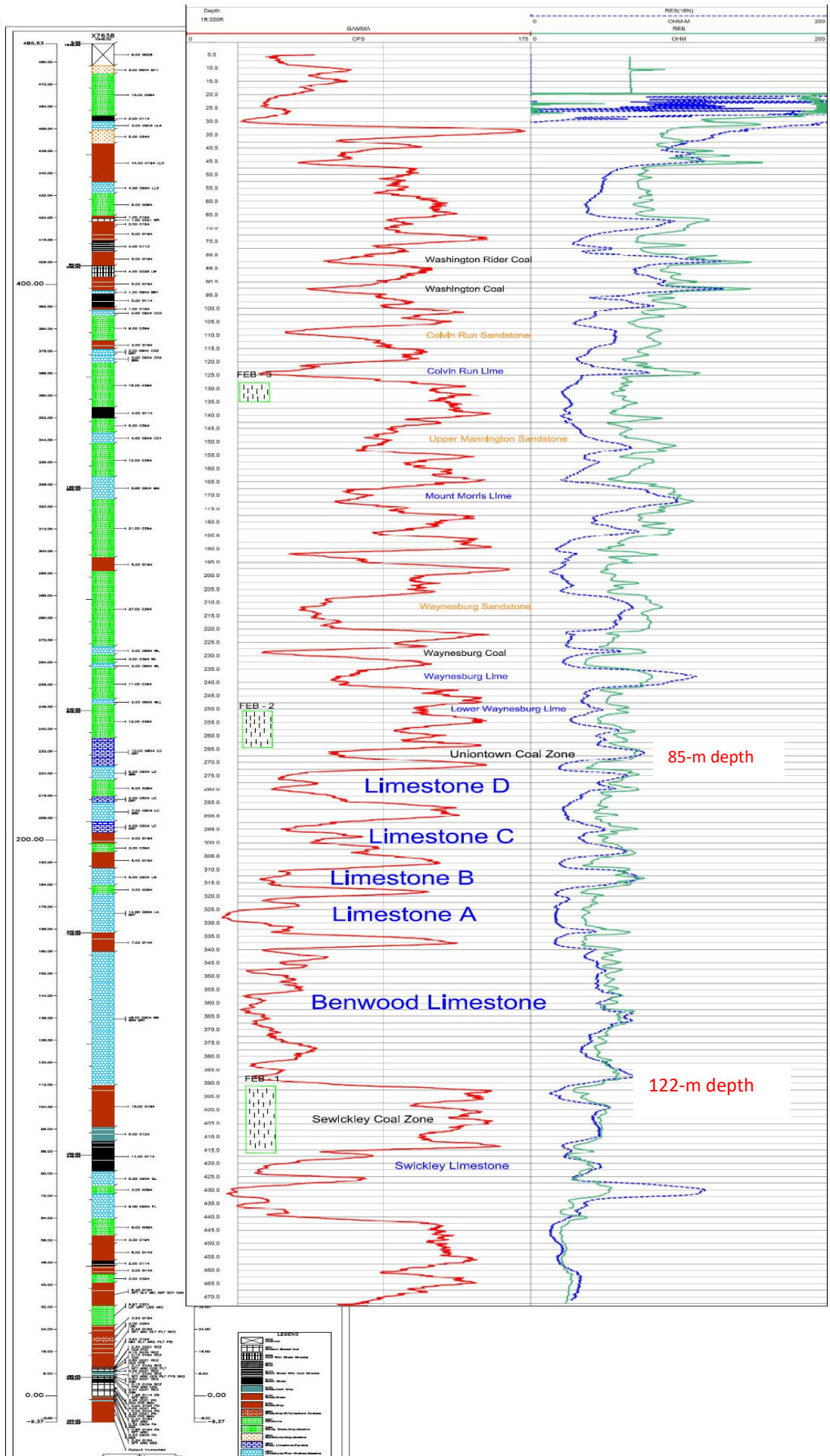

3D FINITE DIFFERENCE SIMULATIONS

A series of FLAC3D finite difference simulations were conducted and analyzed to evaluate the effect of longwall excavations on the induced stresses and deformations within the gate-road abutment pillar. Detailed overburden geology, depicted in Figure 3, was the primary model input. Specifically, over 180 weak-to-strong rock interfaces were present and simulated in the model, which employed over 400,000 zones. A hypo-elastic longwall gob model with a maximum deformation of 25% was employed in the FLAC3D models. The primary goal of the simulations was to duplicate measured surface subsidence, measured subsurface in-place inclinometer displacement, and measured underground coal pillar pressure increase.

RESULTS OF GEOTECHNICAL INSTRUMENTATION AND 3D NUMERICAL ANALYSES

Surface subsidence surveys were conducted when the first panel longwall face was about 220 meters inby the test site, which occurred in mid-June 2018, and when the first panel longwall face was 920 meters outby the test site, which occurred in October 2018. The inclinometer readings and underground coal pillar pressure readings were recorded continuously as the first panel approached and mined by.

Figure 4 shows the results of surface subsidence measurements after completion of the first panel. The measured maximum supercritical subsidence was 1.38 meters or 0.667 times the 2.07-m extraction height. Also, due to the relatively shallow (147-m) cover, the measured vertical subsidence at the monitoring well site was less than 6 mm. Figure 4 also shows that the surface subsidence profile calculated by the FLAC3D model is in good agreement with the measured profile. Figure 5 illustrates the inclinometer casing displacements along the direction of longwall mining from 18.3 to 140 meters below the surface after the first panel extraction. The maximum lateral movement along the direction of longwall mining at the 122-m depth horizon was about 22.8 mm towards the direction of mining. The inclinometer sensors were purposely oriented along the direction of longwall mining in this field study to capture the influence of the east-west regional horizontal stress under the shallow stream valley environment. Figure 6 shows the FLAC3D calculated inclinometer displacements perpendicular to and along the direction of longwall mining. The calculated maximum lateral displacements perpendicular to and along the direction of longwall mining occur at the 122-m depth horizon, and are 168 mm and 18 mm, respectively. The calculated lateral displacements in the direction of longwall mining are in general agreement with the measured inclinometer displacements shown in Figure 5. Although not measured in this field study, the FLAC3D calculated inclinometer displacement perpendicular to the direction of longwall mining is comparable to but slightly higher than a previous inclinometer measurement under 184 meters of cover (Su, 2016), and is one order of magnitude higher than those measured in a 2018 NIOSH study (Su, et al., 2018a, Su, et al., 2018b) under deep (361-m) cover. This is expected since, under deep cover, the mine is at a farther distance from the same measurement horizons, and, thus, has much smaller influence. Also, for the same distance above the mining horizon, the weak-to-strong rock interfaces are subject to higher vertical loads under deep cover, which are expected to hinder lateral displacement. Figure 7 shows the comparison between measured and computed pillar pressure increase resulting from the first panel mining, which indicates excellent agreement between the measured and computed pillar pressure increases.

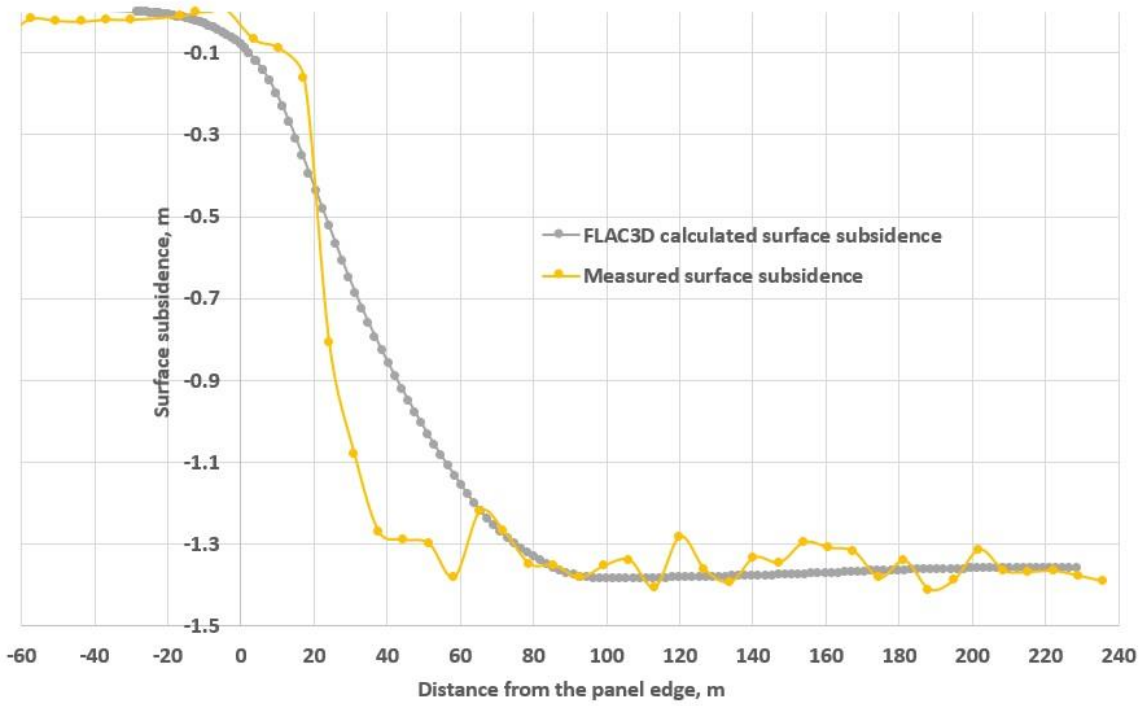

Figure 4. Measured and FLAC3D calculated surface subsidence at the instrumentation site after completion of the first panel.

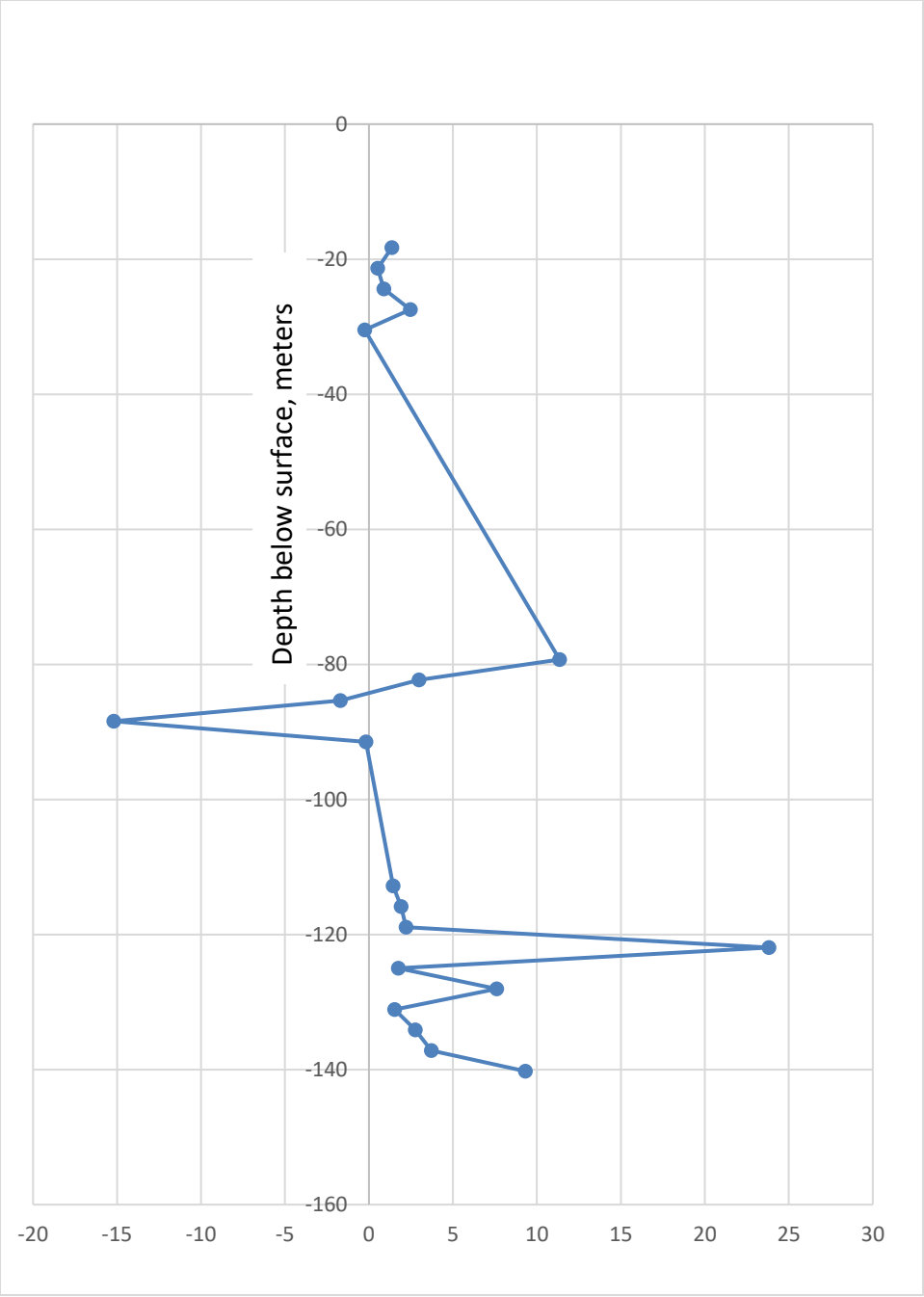

Figure 5. Measured in-place inclinometer displacements after completion of the first panel.

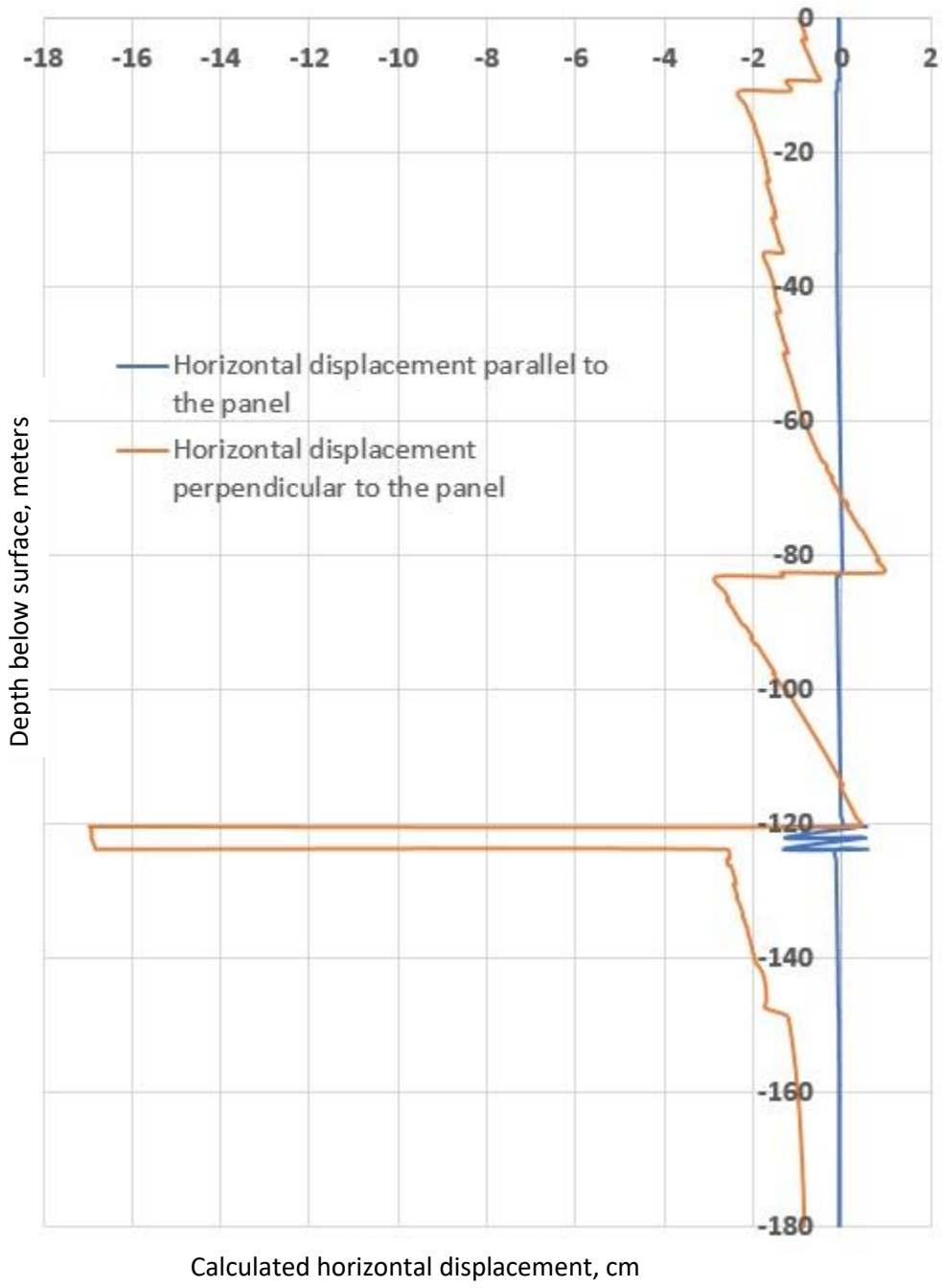

Figure 6. Inclinometer casing displacements perpendicular and parallel to the direction of longwall mining predicted by the FLAC3D model after completion of the first panel.

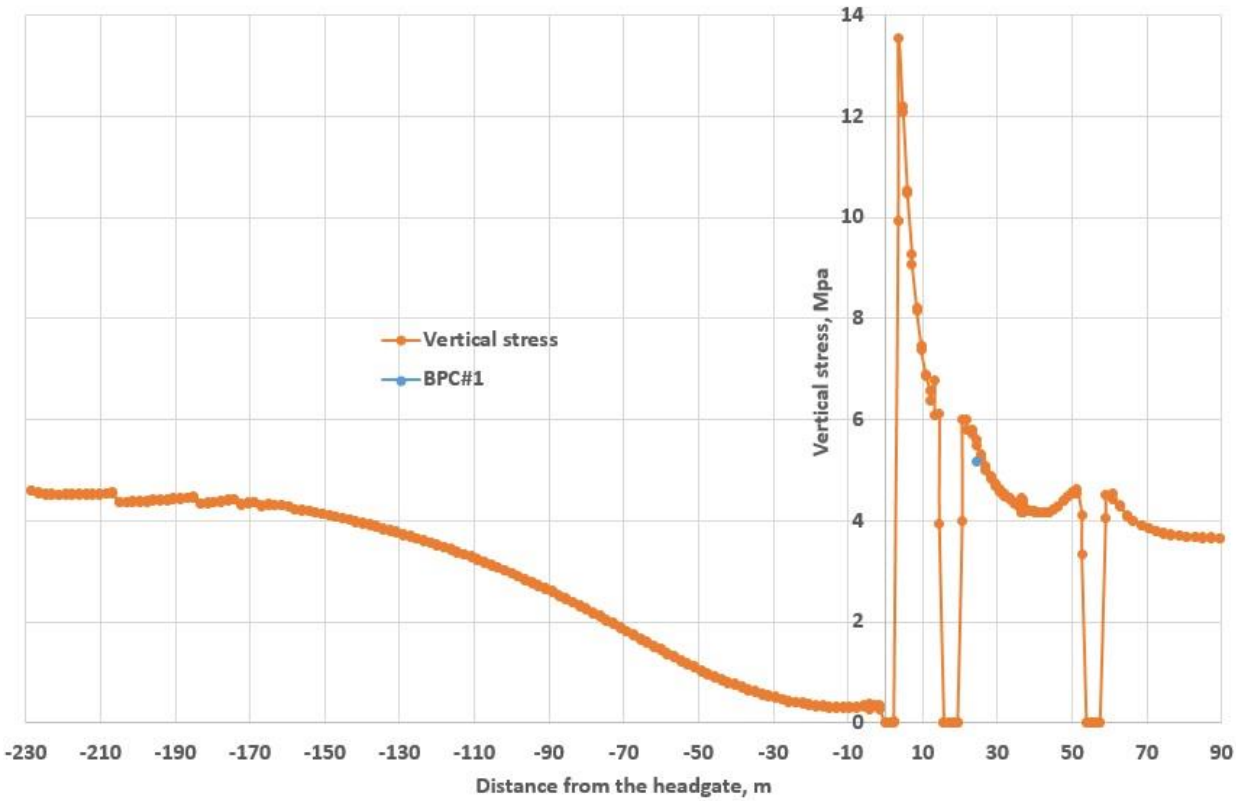

Figure 7. Comparison of measured and computed pillar pressure after completion of the first panel.

RESULTS OF PERMEABILITY MEASUREMENTS AND INTERPRETATION

Permeability testing methodology

As describe in Figure 2, three permeability monitoring holes were drilled adjacent to the inclinometer monitoring hole to measure permeability changes within the abutment pillar as the first longwall approached and mined past the test site. The 125-meter-deep permeability monitoring hole targeted the expected Sewickley Coal Horizon, the 79-meter-deep permeability monitoring hole targeted the Uniontown Coal Zone above the A-, B-, C-, and D-Limestone sequence, and the 41-meter-deep permeability monitoring hole targeted the top of the projected longwall-induced fracture zone.

To meet the objectives of the field study for permeability determinations, a hydrology-based method was used on the three FEB boreholes. The data set consists of changes in water pressure in the boreholes which is converted to a series of water head values. For the measurement of downhole pressure in the three permeability monitoring boreholes, submersible pressure transducers were installed near the bottom of each testing interval. In FEB1, the transducer was positioned at a shallower location but was submersed throughout testing. Slug testing was performed in the boreholes to produce a series of discrete permeability measurements. In addition, the downhole

transducers produced a continuous set of data for permeability determinations in accordance with methodology described by Dawson and Istok (1991).

Results and interpretation

Slug testing for the measurement of permeability within the slotted test sections of the FEB1, FEB2, and FEB3 boreholes was initiated with longwall face 72 meters inby the surface site and continued until the face was over 900 meters past (outby) the site. A total of 11 downhole measurements were conducted during this mine-by phase.

Data from borehole FEB1 is shown in Figure 8. The slug test performed with the face 72 meters inby the borehole site yielded data indicating a permeability of 4.48 X 10^{-13} m^2 for the Sewickley Coal bed horizon. When the longwall face reached a position adjacent to the borehole site, slug testing produced a value of 5.14 X 10^{-13} m^2. At a later time during the mining of the study panel, slug testing was performed with the face 817 meters outby (past) the borehole site. Data acquired from this test indicated a permeability of 1.15 X 10^{-12} m^2.The overall trend in permeability changes for Borehole FEB1, which targets the Sewickley horizon, is an increase to more than double the starting magnitude over the reporting period. Figure 9 shows the permeability test results for Borehole FEB2, which monitored the Uniontown Coal bed horizon. These measurements indicate a permeability of 1.43 X 10^{-13} m^2 when the face was 72 meters inby the test site. The measured permeability increased to 2.04 X 10^{-13} m^2 when the face was adjacent to the test site. With continued mining on the study panel, an increase in permeability to 2.41 X 10^{-13} m^2 was measured in FEB2 with the face 817 outby the test site. These data are intended as a generalized view of permeability magnitude with face position over the reported interval. Results from Borehole FEB3 are shown in Figure 10. The earliest data set shown was acquired when the face was 184 meters outby the borehole site. These data indicated a permeability of 1.47 X 10^{-11} m^2 for the test interval at the anticipated top of the fractured zone formed in the longwall gob. At a later time, with the face 986 meters outby the test site, a slug test was performed indicating an increase in permeability to 2.76 X 10^{-11} m^2. The very rapid losses in water head in FEB3 (Figure 10) may have produced some larger errors in these measurements, which rely on a portion of these values for the permeability calculations. However, the FEB3 test interval certainly produced the highest permeability.

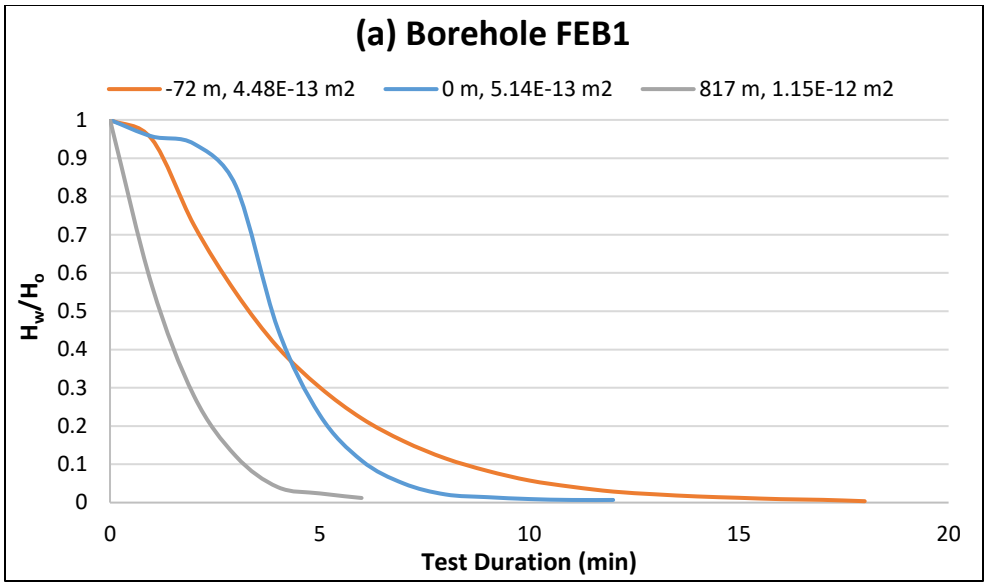

Figure 8. Measured permeability changes in the 125-meter-deep Permeability monitoring hole after first panel mining.

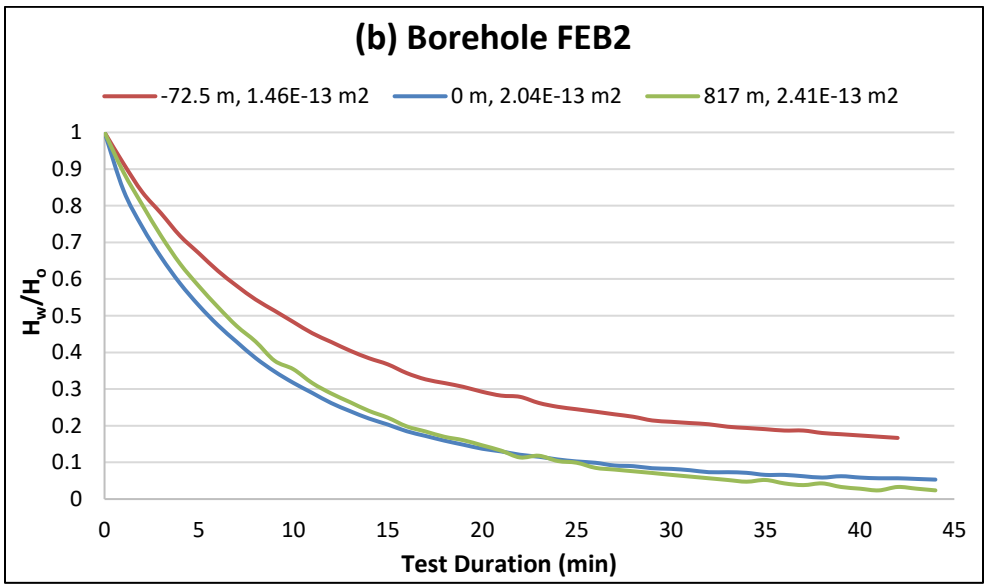

Figure 9. Measured permeability changes in the 79-meter-deep Permeability monitoring hole after first panel mining.

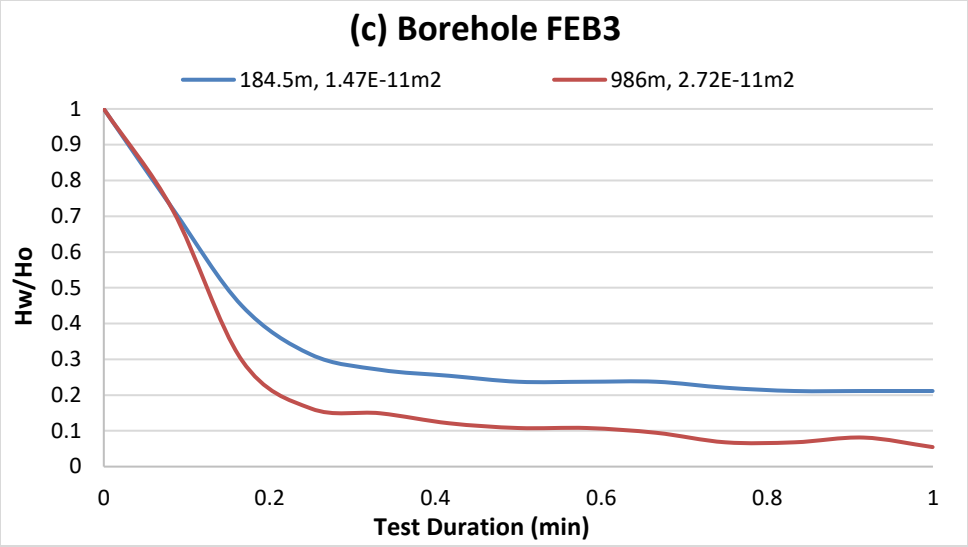

Figure 10. Measured permeability changes in the 41-meter-deep Permeability monitoring hole after first panel mining.

FLAC3D MODELING OF WELL CASING STABILITY UNDER SHALLOW COVER

A number of FLAC3D finite difference models, Figures 11(a) and 11(b), were also constructed to evaluate the potential effects of longwall-induced stresses and deformations within the longwall abutment pillars on shale gas well casing integrity. The overburden geology depicted in Figure 3 was used as the primary inputs for the FLAC3D models.

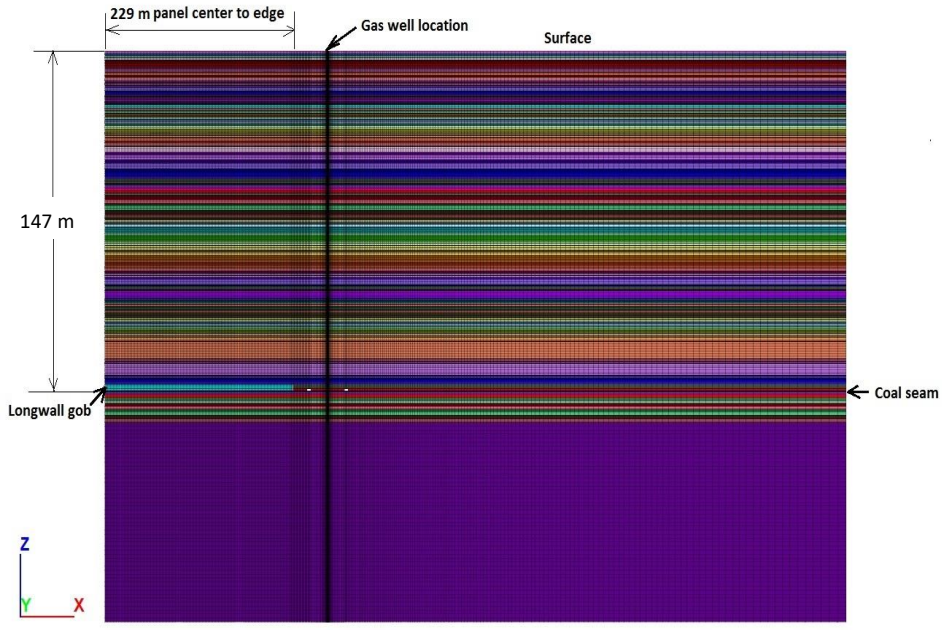

Figure 11(a). 3D finite difference model of a gas well in a longwall abutment pillar.

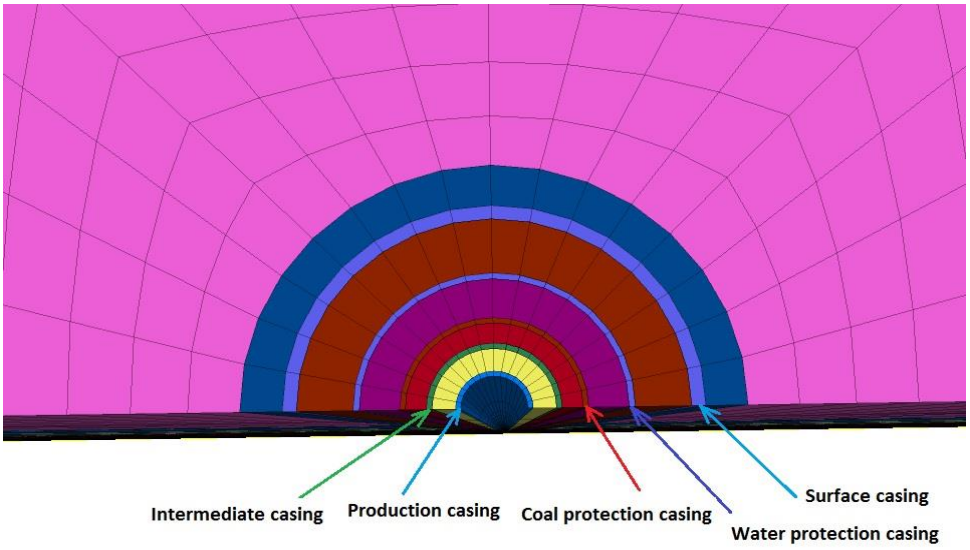

Figure 11(b). Detailed 3D finite difference model of a gas well in a longwall abutment pillar.

It is well known that overburden depth and its associated geology have a significant influence on longwall-induced stresses and deformations. The calibrated FLAC3D models were employed to evaluate the effect of longwall-induced stresses and deformations and their impact on gas well casings under shallow cover and under the influence of a stream valley. Figures 12(a) and 12(b) show that, under shallow overburden and the presence of major soft-to-hard rock interfaces, the longwall-induced deformations caused the coal protection, intermediate, and production casings to deform, and the resulting von Mises stresses in the three casings exceed the yield stresses of the individual casing. In particular, where the maximum lateral deformations coincide with the casing joints, potential leak of the high pressure, high volume gas may occur. To evaluate the path of such potential leak within the longwall abutment pillar and its impact on longwall ventilation as well as miner safety and health, a preliminary calculation of gas inflow was attempted and the results are presented below.

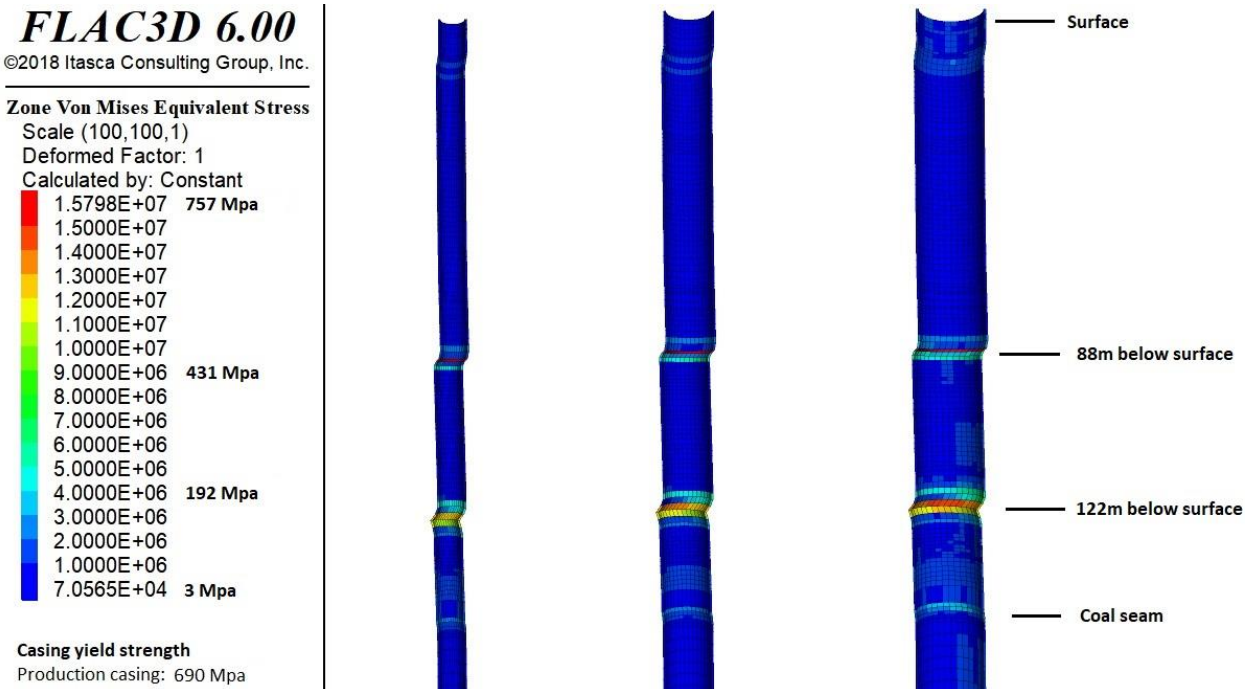

Figure 12 (a). Longwall-induced von Mises stress in the coal protection, intermediate, and production casings (grouted to the surface) under 147 meters of cover.

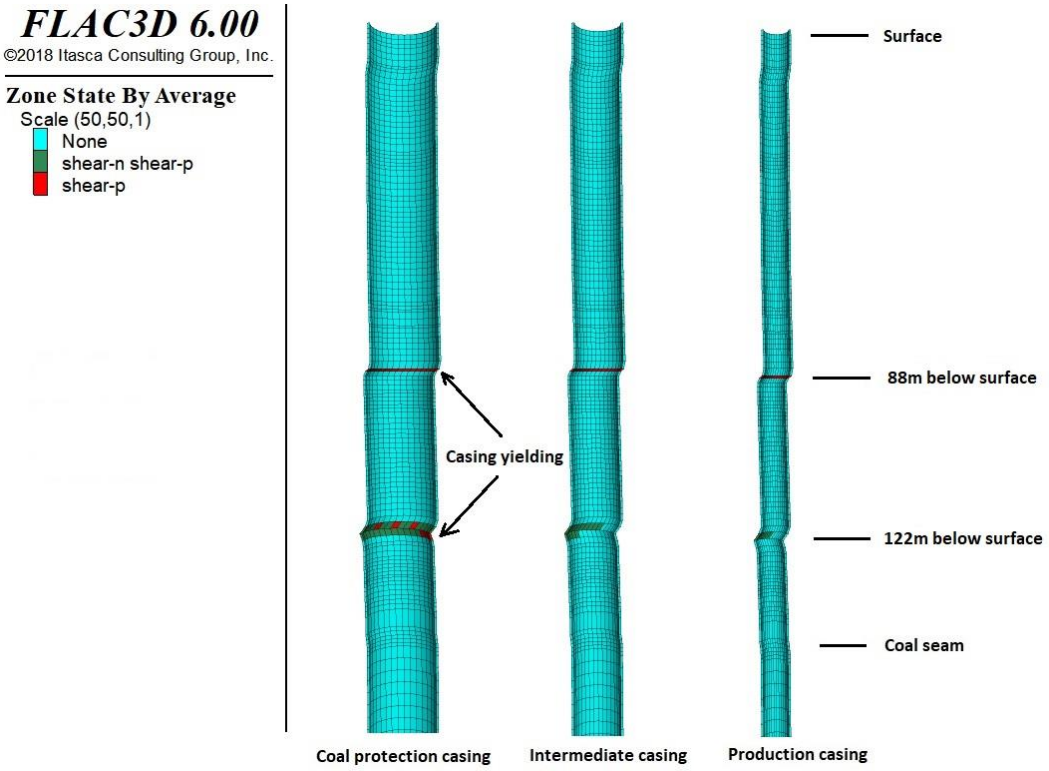

Figure 12 (b). Longwall-induced yielding in the coal protection, intermediate, and production casings (grouted to the surface) under 147 meters of cover.

POTENTIAL GAS RELEASE FROM ENHANCED PERMEAMILITY AFTER FIRST PANEL MINING

To estimate the potential release of natural gas into the active mining zone from shale gas well casings subjected to longwall-induced subsurface deformations, the Darcy's equation (Equation 1) is used. The Darcy equation assumes flow through a porous media results from the pressure gradient across that porous zone in addition to fluid and porous material properties.

$$Q = \frac{kA\Delta P}{\mu L} \quad (1)$$

Where Q is fluid flow rate measured in $m^3/_S$, k is permeability in m^2, ΔP is the pressure gradient across the porous zone in Pascal, μ is the dynamic viscosity of the fluid in Pa s, and L is the characteristic length of the porous media. For the shale gas well scenario, two separate porous zones are assumed for gas transport. The first being the zone of fractured rock between the shale gas well and the longwall caved zone. This porous material has a permeability calculated from a water plug drop down test conducted on Wells FEB#1 and FEB#2 when active mining was 817m outby the well. The second zone is the caved and fractured zone above the longwall panel with a permeability value defined by Esterhuizen et al. (2007). In order to describe fluid flow through multiple porous media, the pressure (P_x) at the interface between the two zones needs defining and is described by Equation (2):

$$P_x = \frac{\frac{P_2 k_2}{L_2} + \frac{P_1 k_1}{L_1}}{\frac{k_2}{L_2} + \frac{k_1}{L_1}} \quad (2)$$

The volumetric flow across both porous zones can then be calculated using Equation (3):

$$Q = \frac{k_2 A(P_x - P_2)}{\mu L_2} \; or \; Q = \frac{k_1 A(P_1 - P_x)}{\mu L_1} \quad (3)$$

The potential gas flow was estimated for two separate scenarios, where the pipe rupture height above the active mining (L_2) changes. The two heights used, 25m and 58.5m, were determined by where the IPI test well displayed the highest horizontal displacement during active mining. Table 1 displays the full set of parameter values for each set of gas release scenarios.

Table 1: Parameter Values for Gas Release Scenarios

Scenario 1									
Characteristic Length L1 (m)	Chararcteristic Length L2 (m)	Permeability K1 (m2)	Permeability K2 (m2)	Cross Sectional Area of Flow (m2)	Dynamic Viscosity Methane μ (Pa s)	Pressure P1 (Pa)	Pressure P2 (Pa)	Pressure Px (Pa)	Volumetric Flow Q (m3/s)
34.9	25	1.30E-12	7.895E-10	0.01156	1.08E-05	2.07E+07	0	24387	**8.24E-04**
Scenario 2									
Characteristic Length L1 (m)	Chararcteristic Length L2 (m)	Permeability K1 (m2)	Permeability K2 (m2)	Cross Sectional Area of Flow (m2)	Dynamic Viscosity Methane μ (Pa s)	Pressure P1 (Pa)	Pressure P2 (Pa)	Pressure Px (Pa)	Volumetric Flow Q (m3/s)
34.9	58.5	2.41E-13	7.895E-10	0.01156	1.08E-05	2.07E+07	0	10586	**1.53E-04**

A shale gas well diameter of 121.4 mm was used for the cross sectional area A. The air pressure in the active mining zone was assumed to be negligible. In both scenarios, the event of the pipe rupture and resulting increased pore pressure are assumed to not influence the permeability of both porous zones. The permeability was set to be constant across each of the porous rock zones. The values for the resulting volumetric fluid flows were $8.24 \times 10^{-4}\ m^3/_S$ and $1.53 \times 10^{-4}\ m^3/_S$, for scenarios 1 and 2, respectively. It is important to note that such a small amount of gas release is not expected to impact the longwall ventilation

system. However, this preliminary calculation only takes into account the effect of first panel mining, where the gob is 35 meters away. With completion of second panel mining, where the gob is only 16.6 meters away, enhanced permeability within the abutment is expected and the amount of gas release is expected to increase.

DISCUSSION

The field instrumentation as well as the numerical modeling results presented in this paper are consistent with a few previous attempts to characterize unconventional subsurface movements along the bedding planes (Su, 1991; Su, 2016; Su, 2018; Su, et al., 2018a; Su, et al., 2018b). Since about 1,500 unconventional shale gas wells have been drilled recently ahead of mining in the Pittsburgh coalfield, and because all casings of these wells are fully cemented to the surface, depending on the distance to the edge of future longwall extraction, potential casing deformation may be present. To avoid sterilizing either coal or gas reserves, these wells need to be temporarily plugged before mining. Upon completion of mining, temporary plugs can be removed and well integrity must be examined and confirmed before returning the wells to production. Over the next few years, it is imperative that research be conducted to define the safeguard distance under various overburden depth and geology, as well as the cementing alternatives to mitigate the effect of longwall-induced subsurface deformations.

CONCLUSIONS

This paper confirms that under shallow cover and under the influence of a major stream valley, longwall-induced subsurface deformations will be one order of magnitude higher than those observed under deep cover. With the presence of major strong-to-soft rock interfaces, large horizontal displacement along these planes of weakness will occur and shale gas well casing integrity may be compromised. Based on the measured permeability increase after first panel mining, the projected gas release from a compromised shale gas well casing is small and is not expected to impact longwall ventilation. However, with second panel mining, the longwall-induced permeability is expected to increase. This paper also demonstrates that the FLAC3D finite difference models, with accurate geologic information and gob behavior, can provide accurate prediction of surface subsidence and underground coal pillar pressure increases. The FLAC3D models can also provide reasonable prediction of complex subsurface strata deformations. Results from this research suggest that numerical models can be used to predict longwall-induced stresses and deformations with reasonable accuracy, as long as they incorporate detailed overburden geology and important strata interface and gob behaviors.

DISCLAIMER

The findings and conclusions in this report are those of the authors and do not necessarily represent the views of the National Institute for Occupational Safety and Health. Mention of any company or product does not constitute endorsement by NIOSH.

REFERENCES

1. Commonwealth of Pennsylvania, Department of Mines and Mineral Industries, Oil and Gas Division. (1957). “Joint Coal and Gas Committee, Gas Well Pillar Study.” Harrisburg, Pennsylvania, 28 pp.
2. Dawson K. J. and J. D. Istok (1991). Aquifer testing: design and analysis of pumping and slug tests. Chelsea, MI: Lewis Publishers, Inc.
3. Esterhuizen, G.S. and C. Karazen (2007). A methodology for determining gob permeability distributions and its application to reservoir modeling of coal mine

longwalls. SME Annual Meeting and Exhibit, Denver, Colorado, 6 pp.

4. **Itasca** Consulting Group Inc. (2017). "FLAC3D Version 6.0".
5. Su, W.H. (1991). Finite element modeling of subsidence induced by underground coal mining: the influence of material nonlinearity and shearing along existing planes of weakness. In: Proc. 10th International Conference on Ground Control in Mining. Morgantown, West Virginia, 287–300.
6. Su, W.H. (2016). Effects of longwall-induced stress and deformation on the stability and mechanical integrity of shale gas wells drilled through a longwall abutment pillar. In: Proceedings of the 35th International Conference on Ground Control in Mining. Morgantown, West Virginia, 119–125.
7. Su, W.H. (2018). Stability of shale gas well casing under the influence of longwall-induced subsurface deformations. Presentation at the 2nd International Conference on Gas, Oil, and Petroleum Engineering, Houston, Texas.
8. Su, W.H., P. Zhang, M. Van Dyke, and T. Minoski (2018a). Effects of cover depth on longwall-induced subsurface deformations and shale gas well casing stability. 52nd ARMA Conference, Seattle, WA, 20 pp.
9. Su, W.H., P. Zhang, M. Van Dyke, and T. Minoski (2018b). Effects of longwall-induced subsurface deformations on shale gas well casing stability under deep covers. In: Proceedings of the 37th International Conference on Ground Control in Mining. Morgantown, West Virginia, 63-70.